LEARNING FINE-GRAINED REPRESENTATIONS THROUGH TEXTUAL TOKEN DISENTANGLEMENT IN COMPOSED VIDEO RETRIEVAL

Anonymous authors
Paper under double-blind review

ABSTRACT

With the explosive growth of video data, finding videos that meet detailed requirements in large datasets has become a challenge. To address this, the composed video retrieval task has been introduced, enabling users to retrieve videos using complex queries that involve both visual and textual information. However, the inherent heterogeneity between modalities poses significant challenges. Textual data is highly abstract, while video content contains substantial redundancy. This modality gap in information representation makes existing methods struggle with the fine-grained fusion and alignment required for fine-grained composed retrieval. To overcome these challenges, we first introduce FineCVR-1M, a fine-grained composed video retrieval dataset containing 1,010,071 video-text triplets with detailed textual descriptions. This dataset is constructed through an automated process that identifies key concept changes between video pairs to generate textual descriptions for both static and action concepts. For fine-grained retrieval methods, the key challenge lies in understanding the detailed requirements. Text descriptions serve as clear expressions of intent, allowing models to distinguish fine-grained needs through textual feature disentanglement. Therefore, we propose a textual Feature Disentanglement and Cross-modal Alignment framework (**FDCA**) that disentangles features at both the sentence and token levels. At the sequence level, we separate text features into retained and injected features. At the token level, an Auxiliary Token Disentangling mechanism is proposed to disentangle texts into retained, injected, and excluded tokens. The disentanglement at both levels extracts fine-grained features, which are aligned and fused with reference video to extract global representations for video retrieval. Experiments on FineCVR-1M dataset demonstrate the superior performance of FDCA.

1 INTRODUCTION

The explosive growth of video data poses a challenge for users seeking videos that meet fine-grained requirements within a vast video database. This demand can be modeled as complex query patterns, *i.e.*, composed video retrieval (CVR) (Ventura et al., 2024; Hummel et al., 2024). CVR combines a reference video and a modification text as a query to find visually similar and semantically relevant videos with altered objects, attributes, or actions. However, existing methods (Ventura et al., 2024; Hummel et al., 2024), including foundational visual-language models(Radford et al., 2021; Li et al., 2022), perform poorly in meeting fine-grained retrieval requirements (Ventura et al., 2024). We identify the primary reason is the semantic granularity gap between textual and visual representations. To address this, we first introduce a new dataset with more detailed and fine-grained textual descriptions. Second, we decompose textual representation for fine-grained fusion and alignment.

Present CVR datasets include CoVR (Ventura et al., 2024) and EgoCRV (Hummel et al., 2024). However, these datasets fail to convey the fine-grained user demands, whereas the modification texts focus solely on the changed element, neglecting to specify the visual information that should remain consistent. This oversight often causes redundant visual information in the reference videos to mislead models. Consequently, the returned videos may contain incorrect visual parts. See the example in Figure 1 (b), the phrase “change to drinking” highlights the action of drinking but fails

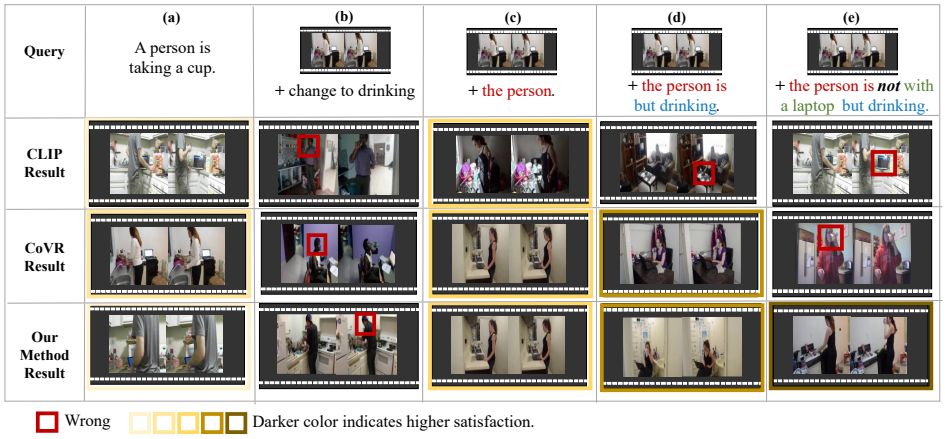

Figure 1: A user wants to retrieve videos of similar people "taking a cup not with a laptop and drinking". (a) In video-text retrieval, the results often fail to meet user expectations from a visual perspective due to the limitations of text queries. (b) In composed video retrieval, focusing on the altered elements is vague, leading to mismatched results. (c)-(e) As the three components are gradually incorporated into the modification text, the retrieved videos become increasingly aligned with the user's intent.

to convey the essential visual context from the reference video. As a result, the returned videos either visually resemble the reference video or simply depict drinking, failing to deliver satisfactory results. Therefore, it is essential to introduce more precise modification texts that explicitly convey fine-grained requirements to enhance retrieval effectiveness.

To facilitate the fine-grained CVR task while minimizing extensive annotating efforts, we highlight the conceptual similarities and differences in text queries and construct a new dataset **FineCVR-1M**, containing over one million triplets. Each triplet consists of a pair of similar videos and modification text that precisely describes the conceptual relevance between the videos. To convey the fine-grained user demands, we generate modification texts based on three components, including **retained component** that remain consistent in the reference and target videos, **injected component** that are newly added in the target videos, and **excluded component** that are expected to be excluded from the target videos. Compared to the simple phrases (Liu et al., 2021; Wu et al., 2021; Ventura et al., 2024; Hummel et al., 2024), modification texts with the three components explicitly express fine-grained user demands on complex video content. Our constructed FineCVR-1M constitutes a total of 1,010,071 triplets encompassing diverse concepts. It can be utilized for developing CVR models and enhancing the fine-grained information-seeking ability of multimodal foundation models.

Given existing coarse-grained CVR datasets, current CVR methods also lack exploration of the finer-grained demands, including our proposed three components (Ventura et al., 2024; Hummel et al., 2024; Thawakar et al., 2024). These methods primarily focus on cross-modal alignment and fusion at the sentence level, leading to highly-coupled feature extraction and inferior performance on the fine-grained CVR task. To address fine-grained retrieval, we propose a Textual Feature Disentanglement and Cross-modal Alignment framework (FDCA). FDCA disentangles modification text at both sentence and token levels, where cross-modal alignment is performed between video and text in a guidance manner. By leveraging both sentence- and token-level semantic analysis, FDCA ensures a more accurate alignment between the text and visual content, ultimately improving the performance of fine-grained CVR.

We compare our method with several composed retrieval methods on the FineCVR-1M dataset. Experimental results demonstrate that our method outperforms existing methods by a clear margin. Our study provides strong support from both dataset and methodology perspectives in enhancing the fine-grained information seek ability of multi-modal video pre-trained models. To summarize, our contribution is threefold:

- We construct a benchmark **FineCVR-1M** with 1M+ triplets. This benchmark supports the combined query with both reference videos and modification text for fine-grained video retrieval and will be made publicly available.

- We propose **FDCA** that performs text feature disentangling at sentence and token levels to progressively enhance the descriptive power of features of the reference video, facilitating efficient retrieval of target videos that visually and semantically satisfy user expectations.
- Extensive experiments show the high quality of FineCVR-1M and the advantage of FDCA.

2 Related Work

Composed Query Dataset requires generating captions for the differences between the reference and target videos. Recently, two CVR datasets have emerged: CoVR (Ventura et al., 2024) and EgoCRV (Hummel et al., 2024). CoVR employs a large language model (LLM) (Touvron et al., 2023a) to generate captions highlighting the differences between two reference captions, while EgoCRV manually creates a test set for first-person perspective videos. However, the modification texts in both datasets do not explicitly describe fine-grained requirements, leading to an inability to support fine-grained CVR tasks. In our work, we construct datasets by employing clear textual prompts and the LLM to automatically generate detailed text descriptions based on video content, thereby supporting fine-grained composed retrieval.

Composed Image Retrieval (CIR) aims to get the target image by a composed query including a reference image and modification text. Current CIR models mainly focus on feature discrimination and feature composition. Discriminating features requires distinguishing the retained features in the reference images and the features need to be injected into the target image. Present methods employ gate mechanism (Vo et al., 2019) or semantic-guided attention mechanism (Chen et al., 2020b; Lee et al., 2021; Wen et al., 2021; Hosseinzadeh & Wang, 2020; Baldrati et al., 2023; Saito et al., 2023) to discriminate these features. The feature composition is addressed by projecting visual and textual features into a common space, often utilizing a cross-modal Transformer (Saito et al., 2023; Baldrati et al., 2023). However, due to a lack of temporal information, these CIR methods can only be applied to static modifications and cannot be extended to CVR directly.

Composed Video Retrieval (CVR) extends the concept of composed retrieval from the image domain to the video domain. The CoVR (Ventura et al., 2024) employ the BLIP (Li et al., 2022) directly to achieve cross-modal alignment and fusion, while EgoCVR uses a train-free reranking approach. To obtain the enhanced semantics from modification text, (Thawakar et al., 2024) leverages an LLM to enrich modification texts. However, these methods emphasize coarse-level feature alignment. Additionally, WTI (Wang et al., 2022) in video-text retrieval incorporates weighted token interaction for fine-grained feature alignment. However, it does not consider the specific semantics of tokens, especially when text plays a crucial role in CVR. In contrast, our FDCA focuses on discriminating textual features into three meaningful components for fine-grained CVR.

3 FineCVR-1M Dataset Construction

Items in the dataset are organized as triplets $\{\mathcal{V}_\mathrm{r}, \mathcal{T}, \mathcal{V}_\mathrm{t}\}$, where $\mathcal{T}$ denotes the modification text describing the differences between a reference video $\mathcal{V}_\mathrm{r}$ and a target video $\mathcal{V}_\mathrm{t}$. We first match similar videos as the reference video and the target video, then generate modification texts automatically. For the static concepts, modification texts are generated by filling different and similar key static concepts into the textual prompts. For action concepts, we directly employ a fine-tuned LLM to generate descriptions of the action differences and similarities.

3.1 Video Preprocessing and Pairing

To ensure diversity and accuracy, we first collect videos from easily accessible datasets. We use four datasets, ActionGenome (Ji et al., 2020), ActivityNet (Fabian Caba Heilbron & Niebles, 2015), HVU (Diba et al., 2020), and MSRVTT (Xu et al., 2016) as our video source. These videos provide rich information on the visual contents, such as actions, scenes, objects, and attributes. To reduce the redundancy of the videos, we clip videos into different events based on their temporal boundary annotations and remove videos lacking corresponding captions.

To match similar video pairs that contain slightly different content, following (Chen et al., 2020a; Xu & Wang, 2021), we compute the cosine similarity between the BLIP-2 features (Li et al., 2023)

Table 1: Statistics of FineCVR-1M compared to existing CVR datasets. "RC" denotes "Retained Component", "IC" denotes "Injected Component", and "EC" denotes "Excluded Component". FineCVR-1M enhances various objectives with fine-grained components for precise descriptions.

	Train triplets	Test triplets	Visuals	Unique word	Attribute-Centric	Object-Centric	Scene-Centric	Action-Centric	RC	IC	EC
WebVid-CoVR	1,648,789	2,556	133,219	21,098	-	85.0%	-	15.0%		✓	
EgoCVR	-	2,295	2,295	940	-	21.1%	-	78.9%		✓	
FineCVR-1M	1,000,028	10,043	136,547	20,961	0.5%	22.1%	28.5%	48.9%	✓	✓	✓

of videos and select the top 20 most similar matches for each video. Pairing videos facilitates the comparison of video content and generating their corresponding modification texts.

3.2 Modification Text Generation

3.2.1 Static Concepts

Basic Static Concept Detection. Static concepts, in contrast with the action concepts of the objects, refer to contents such as objects, attributes, and scenes. Basic static concepts in the videos serve as the flags for identifying both the content differences between videos and the contents of query interests. To ensure a comprehensive detection of the static concepts, we extract them from both video frames and their annotations. The former are often visually salient concepts, while the latter are high-quality and semantically significant.

Key Static Concept Selection. In this step, we assign scores for concepts of each video clip to identify key concepts. Specifically, concepts from annotations, created by humans, are considered highly credible and align with human attention, obtaining higher scores. In contrast, concepts from video frames may contain error and noise, obtaining lower scores. Based on the assigned scores, we select key static concepts with the top 5 highest scores in each type for every video. An example is shown in the Appendix Figure A9.

Modification Text Generation. We compare key static concepts between video pairs and generate descriptions of their differences with three types of prompts. Details are in the Appendix B.2.

3.2.2 Action Concepts

In addition to the static video concepts, we also generate modification texts regarding the fine-grained action differences by fine-tuning LLaMA2 (Touvron et al., 2023b). Specifically, we construct a prompt (further elaborated in Appendix B.2) to instruct the ChatGPT (Ouyang et al., 2022) to generate text that describes the action differences between caption annotations. The generated descriptions are manually corrected for the fine-tuning of LLaMA2 with LoRA (Hu et al., 2021). We apply the fine-tuned LLaMA2 to the matched similar video pairs and produce descriptions of the action differences between videos.

3.3 Dataset Property

FineCVR-1M consists of 1,000,028 training triplets and 10,043 test triplets. Detailed statistics are presented in Table 1. Given the unavoidable noise in the automatic construction process, we manually select triples with accurate ground-truth modification text descriptions as the test subset for evaluation. Although our triplet count is lower than that of WebVid-CoVR, FineCVR-1M has a larger number of videos and comparable richness of the descriptive texts. In comparison with the other two CVR datasets that focus only on objects and actions, FineCVR-1M targets four categories (attribute, object, scene, and action) for modification and retains three crucial components (**retained component**, **injected component**, and **excluded component**) in the modification texts, enabling fine-grained video retrieval. More analyses of FineCVR-1M are shown in Appendix B.3.

4 Method

Given a pair of reference video and modification text $\{\mathcal{V}_r, \mathcal{T}\}$ as query, CVR requires cross-modal alignment to relate the composed query fusion feature with a video feature. This fusion feature can

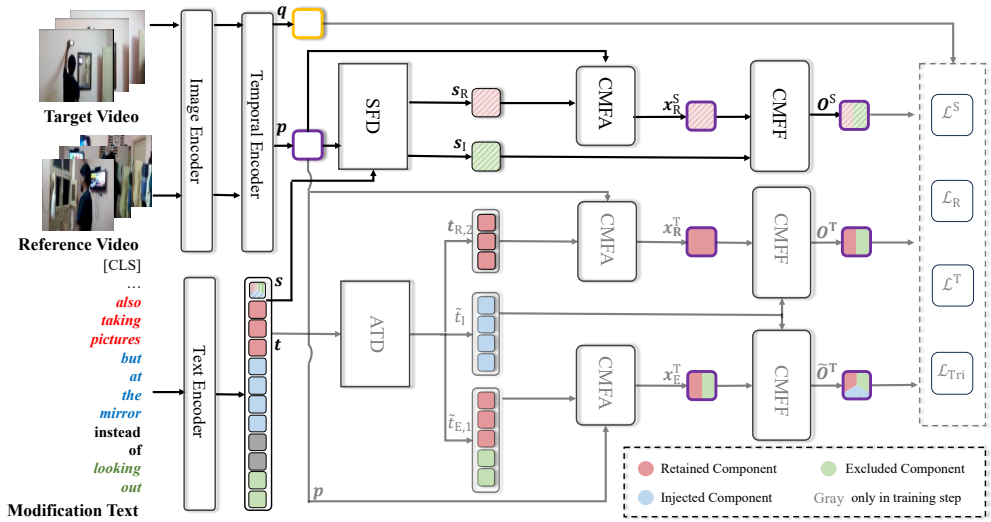

Figure 2: Overall pipeline of FDCA involves fine-grained cross-modal alignment and fusion through the disentangling of text features. We further enhance this process by introducing token-level disentangling, where clustering is used to generate three types of features, enabling the model to focus on fine-grained information.

be employed to retrieve the target video $\mathcal{V}_{\mathrm{t}}$ from the video database, which should satisfy both visual and semantic demands. As shown in Figure 2, to capture fine-grained user demand, we propose a Textual Feature Disentanglement and Cross-modal Alignment framework (FDCA), disentangling modification text at both sentence and token levels. Specifically, Sentence-level Feature Disentangling (SFD) is proposed to disentangle the text feature into the retained and injected components, followed by the Cross-modal Feature Alignment (CMFA) and Cross-modal Feature Fusion (CMFF). At the token level, we introduce Auxiliary Token Disentangling (ATD) during training. ATD clusters token-level features, disentangling tokens into three types of components. These disentangled tokens are used in three auxiliary loss functions to guide the alignment and fusion process, resulting in a semantically enriched video feature for more accurate retrieval.

4.1 Sentence-level Disentanglement and Fusion

The SDF aims to obtain a global fused video feature through modification text feature disentangling and cross-modal fusion.

Video and Text Encoding. Given a video with f frames, we first employ an image encoder (Radford et al., 2021; Li et al., 2022) to extract the reference frame features. The features are then fed into a temporal encoder and integrated as the reference video feature $\boldsymbol{p} \in \mathbb{R}^{1\times d}$. For the modification text of length l that corresponds to the video, a text encoder (Radford et al., 2021; Li et al., 2022) is deployed to extract the sentence-level text feature $\boldsymbol{s} \in \mathbb{R}^{1\times d}$.

Sentence-level Feature Disentangling. Based on the semantic similarity between the modification text and reference video, we design a cross-attention strategy that is guided by the reference video feature. It extracts the retained component from the modification text regarding the reference video. Specifically, we project $\boldsymbol{p}$ and $\boldsymbol{s}$ into the latent space as query, key, and value: $\boldsymbol{Q} = \Psi_{\mathrm{Q}}(\boldsymbol{p}), \boldsymbol{K} = \Psi_{\mathrm{K}}(\boldsymbol{s}), \boldsymbol{V} = \Psi_{\mathrm{V}}(\boldsymbol{s})$, where Ψ_{Q}, Ψ_{K}, Ψ_{V} are implemented as linear layers. Then, the retained text feature $\boldsymbol{s}_{\mathrm{R}} \in \mathbb{R}^{1\times d}$ is calculated by the reference-guided cross-attention $\boldsymbol{s}_{\mathrm{R}} = \mathrm{softmax}(\frac{\boldsymbol{Q}\boldsymbol{K}^{\top}}{\sqrt{d}})\boldsymbol{V} + \boldsymbol{V}$. We assign the remaining features in $\boldsymbol{s}$ as injected text feature $\boldsymbol{s}_{\mathrm{I}} = \boldsymbol{s} - \boldsymbol{s}_{\mathrm{R}}$, which is the newly added semantic content in the target video.

Cross-modal Feature Fusion. The target video feature should capture the retrained feature in the reference video and fuse with the injected text feature. To align the retained text feature with the reference video feature, we input the concatenation of $\boldsymbol{p}$ and $\boldsymbol{s}_{\mathrm{R}}$ into the Cross-modal Feature Alignment module, implemented by a Transformer encoder. This module captures the sentence-level retained component feature $\boldsymbol{x}_{\mathrm{R}}^{\mathrm{S}}$ for the reference video. To further fuse with the injected text

feature, the Cross-modal Feature Fusion, achieved by another Transformer encoder and a linear layer, integrates $\boldsymbol{x}_{\mathrm{R}}^{\mathrm{S}}$ and $\boldsymbol{s}_{\mathrm{I}}$ to produce the global fused video feature $\boldsymbol{o}^{\mathrm{S}}$.

Metric Learning. We employ the contrastive loss to calculate the distance between the global fused video feature $\boldsymbol{o}^{\mathrm{S}}$ and candidate video features in the database:

$$\mathcal{L}^{\mathrm{S}} = -\frac{1}{|\mathcal{B}|}\sum_{i\in\mathcal{B}}\log\frac{\exp\left(\boldsymbol{o}_i^{\mathrm{S}}\boldsymbol{q}_i^{\top}\right)}{\sum_{j\in\mathcal{B}}\exp\left(\boldsymbol{o}_i^{\mathrm{S}}\boldsymbol{q}_j^{\top}\right)}, \tag{1}$$

where the $\boldsymbol{q}_i$ is the candidate video feature. $\mathcal{B}$ is the batch set.

4.2 Token-level Disentanglement and Fusion

Compared to the highly-coupled global sentence-level features, token features with more specific concept information are easier to disentangle. Shown in Figure 3, we use clustering to separate token features into retained, injected, and excluded components, enabling more effective capture of the fine-grained details.

Token Feature Extraction. The token feature $\boldsymbol{t} \in \mathbb{R}^{l\times d}$ is encoded with the text encoder from the original text. Moreover, we also generate positive text by removing negation words like "instead of". Given the positive texts, the text encoder gives rise to the positive text feature $\tilde{\boldsymbol{t}} \in \mathbb{R}^{(l-n)\times d}$, where n denotes the number of negation words.

Auxiliary Token Disentangling. To distinguish the encoded token-level features as different components, we adopt the Density Peaks Clustering based on K-Nearest-Neighbors (DPC-KNN) (Du et al., 2016), a robust clustering technique commonly utilized for tokens clustering (Jin et al., 2023a;b; Zeng et al., 2022). Specifically, given tokens of the modification text, to ensure tokens in each cluster have the same component type, we first apply a one-dimensional convolutional layer across the word sequence. Then we use the DPC-KNN to identify the two centers of the tokens. The remaining tokens are classified into two sets based on the Euclidean distance from the cluster centers. We then average the tokens within each cluster to derive two cluster features.

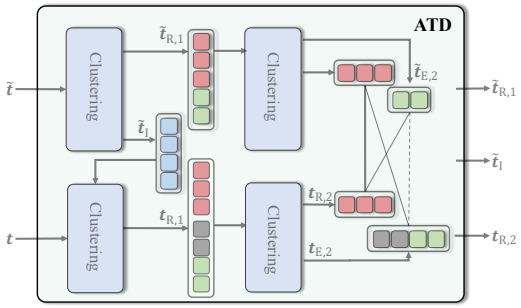

Figure 3: The ATD mechanism.

To identify the injected component, we first note that compared to the original modification text, the positive text is regarded to employ affirmative descriptions, and is thus more semantically similar to the reference video. Therefore, during the component disentanglement at the token level, we apply clustering to the positive tokens $\tilde{\boldsymbol{t}}$ under the guidance of the reference video feature $\boldsymbol{p}$. The clustering gives rise to the positive cluster features $\tilde{\boldsymbol{f}}_1 \in \mathbb{R}^{2\times d}$ of two centers. The features of the cluster centers are then aggregated based on their similarity with the reference video feature $\boldsymbol{p}$. Specifically, this aggregation guided by the reference video learns the initial retained token feature $\tilde{\boldsymbol{t}}_{\mathrm{R},1}$ from the positive text:

$$\tilde{\boldsymbol{t}}_{\mathrm{R},1} = \mathrm{softmax}(\beta\mathrm{sim}(\boldsymbol{p}, \tilde{\boldsymbol{f}}_1)) \cdot \tilde{\boldsymbol{f}}_1, \tag{2}$$

where $\mathrm{sim}(\cdot)$ is dot product similarity, $\mathrm{softmax}$ with β is used to compute a soft index of the maximum similarity. Then we can obtain the injected token feature from the positive text as $\tilde{\boldsymbol{t}}_{\mathrm{I}} = \tilde{\boldsymbol{t}} - \tilde{\boldsymbol{t}}_{\mathrm{R},1}$.

For obtaining the retained and excluded components, note that initial retained tokens generated from the reference video may contain excluded tokens. To address this, we further disentangle the initial retained tokens and get the retained and excluded token features. Specifically, the positive texts and the original texts contain reciprocal information about the excluded component. Therefore, we can first derive the initial retained tokens in the original text and cluster these tokens into two clusters. By comparing the clusters between the original text and the positive text, the most similar pair of clusters belongs to the retained component while the other pair belongs to the excluded component.

Following the clustering on the positive text, we also obtain the cluster features $\boldsymbol{f}_1 \in \mathbb{R}^{2\times d}$ on the original text. The original modification text has similar injected components with its positive counterpart. Therefore, the injected token features from the positive texts $\tilde{\boldsymbol{t}}_{\mathrm{I}}$ can serve as a substitute for the original texts, extracting the initial retained token feature $\boldsymbol{t}_{\mathrm{R},1}$ from $\boldsymbol{f}_1$ through:

$$\boldsymbol{t}_{\mathrm{R},1} = \left[1 - \mathrm{softmax}\left(\beta \mathrm{sim}\left(\tilde{\boldsymbol{t}}_{\mathrm{I}}, \boldsymbol{f}_1\right)\right)\right] \cdot \boldsymbol{f}_1. \tag{3}$$

Next, we further cluster the initial retained tokens $\tilde{\boldsymbol{t}}_{\mathrm{R},1}$ and $\boldsymbol{t}_{\mathrm{R},1}$, resulting two pairs of clusters $\boldsymbol{f}_2 \in \mathbb{R}^{2\times d}$ and $\tilde{\boldsymbol{f}}_2 \in \mathbb{R}^{2\times d}$. Each constitutes a cluster of clean retained tokens and a cluster of excluded tokens. The clusters of clean retained tokens are more similar to each other. In contrast, the cluster of excluded tokens from the original text is accompanied by negation words, reciprocal to that from the positive text. To distinguish the clusters, similarities between the pairs of clusters are compared, resulting in the clean retained tokens $\boldsymbol{t}_{\mathrm{R},2}$ and the excluded tokens $\tilde{\boldsymbol{t}}_{\mathrm{E},2}$:

$$\boldsymbol{t}_{\mathrm{R},2} = \sum\nolimits_{i=1}^{2} \mathrm{softmax}(\beta\, \mathrm{sim}(\boldsymbol{f}_2, \tilde{\boldsymbol{f}}_2))_i \cdot \boldsymbol{f}_2, \tag{4}$$

$$\tilde{\boldsymbol{t}}_{\mathrm{E},2} = \left[1 - \sum\nolimits_{i=1}^{2} \mathrm{softmax}(\beta\, \mathrm{sim}(\boldsymbol{f}_2, \tilde{\boldsymbol{f}}_2))_i\right] \cdot \tilde{\boldsymbol{f}}_2, \tag{5}$$

where i is the index of the two clusters.

Auxiliary Loss Construction. Given the disentangled fine-grained components at the token level, we further propose an auxiliary loss to ensure the model focuses on the fine-grained information. Resembling the sentence-level feature alignment and fusion, we also apply the CMFA and CMFF modules to the token-level features. For the feature alignment, CMFA aligns clean retained tokens $\boldsymbol{t}_{\mathrm{R},2}$ with the reference video, giving rise to the token-level retained component feature $\boldsymbol{x}_{\mathrm{R}}^{\mathrm{T}}$. For the feature fusion, CMFF fuses $\boldsymbol{x}_{\mathrm{R}}^{\mathrm{T}}$ with the injected positive tokens $\tilde{\boldsymbol{t}}_{\mathrm{I}}$, generating the fused video feature $\boldsymbol{o}^{\mathrm{T}}$. Similar to the Equation 1, the token-level contrastive loss $\mathcal{L}^{\mathrm{T}}$ is calculated between the token-level fused feature $\boldsymbol{o}^{\mathrm{T}}$ with the candidate video feature $\boldsymbol{q}$ to learn fine-grained token-level features following as:

$$\mathcal{L}^{\mathrm{T}} = -\frac{1}{|\mathcal{B}|} \sum_{i\in\mathcal{B}} \log \frac{\exp\left(\boldsymbol{o}_i^{\mathrm{T}} \boldsymbol{q}_i^{\top}\right)}{\sum_{j\in\mathcal{B}} \exp\left(\boldsymbol{o}_i^{\mathrm{T}} \boldsymbol{q}_j^{\top}\right)}, \tag{6}$$

For the finer control at the token level, we propose a contrastive loss to regularize the consistency of the retained components with the reference video. It constrains the distance between the positive retained tokens $\tilde{\boldsymbol{t}}_{\mathrm{R},1}$ and reference video feature $\boldsymbol{p}$ as:

$$\mathcal{L}_{\mathrm{R}} = -\frac{1}{|\mathcal{B}|} \sum_{i\in\mathcal{B}} \log \frac{\exp\left(\tilde{\boldsymbol{t}}_{\mathrm{r},1,i} \boldsymbol{p}_i^{\top}\right)}{\sum_{j\in\mathcal{B}} \exp\left(\tilde{\boldsymbol{t}}_{\mathrm{r},1,i} \boldsymbol{p}_j{}^{\top}\right)}. \tag{7}$$

We also adopt the excluded component to generate negative samples and regularize the negation semantics in the target video. Although there are clean excluded tokens $\tilde{\boldsymbol{t}}_{\mathrm{E},2}$, to avoid the information degradation caused by merging with $\boldsymbol{t}_{\mathrm{R},2}$, we use the initial retained tokens $\tilde{\boldsymbol{t}}_{\mathrm{R},1}$ which contains both retained and excluded components to align with $\boldsymbol{p}$ from the reference database through CMFA. The feature of the identified reference video $\boldsymbol{x}_{\mathrm{E}}^{\mathrm{T}}$ is then fused with $\tilde{\boldsymbol{t}}_{\mathrm{I}}$ in CMFF, obtaining the negative fused video feature $\tilde{\boldsymbol{o}}^{\mathrm{T}}$. We employ the triplet loss $\mathcal{L}_{\mathrm{Tri}}$ to penalize the presence of negation semantics in videos with margin m:

$$\mathcal{L}_{\mathrm{Tri}} = \max(0, m + d(\boldsymbol{q}, \boldsymbol{o}^{\mathrm{T}}) + d(\boldsymbol{q}, \tilde{\boldsymbol{o}}^{\mathrm{T}})), \tag{8}$$

where $d(\cdot)$ represents the distance metric between the two features.

4.3 Overall Loss

The overall loss function is defined as the combination of sentence-level contrastive loss, token-level contrastive loss, constraint loss, and triplet loss:

$$\mathcal{L} = \mathcal{L}^{\mathrm{T}} + \mathcal{L}^{\mathrm{S}} + \mathcal{L}_{\mathrm{R}} + \lambda \mathcal{L}_{\mathrm{Tri}}, \tag{9}$$

where λ is the weight of the triplet loss. With the help of the three additional losses with clear components, the framework can focus on both global and fine-grained information. This comprehensive objective function enhances the model's capability to identify relevant information in the reference video, ensuring that the fused video features align more accurately with the modification texts.

Table 2: Performance on our dataset compared with baseline and existing methods.

Method	Backbone	R1	R5	R10	R50
Video-only	CLIP	8.27	27.89	40.69	70.00
Text-only	CLIP	2.86	9.19	14.61	34.15
Video-text sum	CLIP	8.47	24.85	46.08	65.01
Linear layer	CLIP	14.68	41.42	57.82	88.74
Linear layer	BLIP	19.13	51.79	68.60	93.62
TIRG (Vo et al., 2019)	Resnet	0.00	25.80	41.20	75.92
Artemis (Delmas et al., 2022)	Resnet	4.76	17.81	28.39	57.92
CosMo (Lee et al., 2021)	Resnet	7.82	25.38	37.45	70.96
MAAF (Dodds et al., 2020)	CLIP	2.16	20.61	33.37	70.39
Uncertainty-R (Chen et al., 2022)	CLIP	5.23	18.45	28.28	60.78
Pic2word (Saito et al., 2023)	CLIP	8.10	25.79	38.32	71.01
TFR-CVR (Hummel et al., 2024)	CLIP	15.21	40.12	52.78	81.75
Combiner (Baldrati et al., 2022)	CLIP	19.57	49.46	65.38	92.11
FreestyleRet (Li et al., 2024)	CLIP	20.39	52.98	68.37	93.03
CoVR (Ventura et al., 2024)	BLIP	17.05	41.57	56.60	85.56
FDCA-CLIP	CLIP	25.84	55.84	70.23	94.33
FDCA-BLIP	BLIP	**26.79**	**63.21**	**78.65**	**97.25**

5 EXPERIMENTS

5.1 EXPERIMENTAL SETUP

All the experiments are conducted on FineCVR-1M with recall at k as evaluation metric. We reproduce several composed retrieval methods including CIR and CVR paradigm. Our image encoder is initialized with both CLIP (Radford et al., 2021) and BLIP (Li et al., 2022) weights. Mean-pooling is used as temporal encoder in all CIR methods, including our FDCA, to ensure fair comparisons.

5.2 COMPARISON RESULTS

Comparison results between our method and both the baseline group and Composed Image/Video Retrieval methods group are shown in Table 2.

Comparison with the pre-trained models. To demonstrate the capability of pre-trained models for CVR task, we set up several baselines with CLIP feature, including utilizing only the reference video feature, utilizing only modification text feature, summing the video feature and text features directly. The fourth and fifth baselines indicate a linear layer trained for fusing cross-modal features with CLIP and BLIP, respectively. Our method significantly outperforms the above five baseline methods, emphasizing the importance of the combined query. Moreover, the score of video-only baseline surpasses that of the video-text sum baseline, indicating simple feature summation cannnot deal with the complex the CVR task, due to the potential misunderstanding and misrepresentation of the modification texts. In contrast, our FDCA focuses on disentangling the modification text regarding the reference video at both sentence and token levels, facilitating more elegant semantic component extraction and alignment in the combined queries.

Comparison with Existing Methods. Our proposed approach demonstrates superior performance, thanks to the disentangling of both global and fine-grained information in our FDCA. Notably, approaches such as Artemis, underperform the baseline methods because no large-scale pre-trained model is used. Moreover, it is worth highlighting that our FDCA-CLIP even outperforms the CoVR method fine-tuned with BLIP. This observation indicates that a well-designed feature disentanglement pipeline is crucial in the CVR task, which, in a sense, appears to be more important than updating to a stronger large-scale pre-trained model.

5.3 ABLATION STUDIES

We conduct ablation studies to assess the necessity of each component in our model on the FineCVR-1M test set. We use CLIP as the image encoder for the case study, and similar observations can also be obtained on BLIP.

Ablation Studies on SFD and ATD. Table 3 shows that our FDCA method leverages the strengths of both SFD and ATD. The approach without disentangling performs poorly due to misinterpreted combined queries. While introducing SFD helps, it still lacks fine-grained information modeling. The method with ATD excels in R1 by focusing on fine-grained details, but it neglects global information, leading to weaker performance in R5, R10, and R50. By combining ATD and SFD, our model effectively balances global and fine-grained information, achieving strong results across all metrics. Moreover, within our FDCA framework, we implement CMFA and CMFF separately using distinct Transformers. When we replace these with a unified Transformer, denoted as " w/ a Trans", we find that the alignment-fusion-separate approach is more effective. This suggests that aligning the retained information before merging it with the retained features allows the model to focus more effectively on the relevant components.

Table 3: Ablation studies on each module.

Method	SFD	ATD	R1	R5	R10	R50
w/o disent			22.03	53.22	69.32	94.33
w/ SFD	✓		22.76	53.20	68.40	94.19
w/ ATD		✓	25.77	50.94	64.46	90.32
w/ a Trans	✓	✓	24.08	54.83	**70.83**	**94.75**
FDCA	✓	✓	**25.84**	**55.84**	70.23	94.33

Ablation Studies on Loss Functions. In Table 4, each loss function contributes to FDCA, resulting in a well-balanced performance across all metrics. Specifically, the method employing $\mathcal{L}^{\mathrm{S}}$ solely focuses on global sentence-level feature disentangling, showing lower scores at R1. Conversely, the method only utilizing $\mathcal{L}^{\mathrm{T}}$ fails to obtain clean components, leading to the lowest performance. By further introducing the $\mathcal{L}_{\mathrm{R}}$ and $\mathcal{L}_{\mathrm{Tri}}$, the fusion module can extract fused features that align with the retained and injected components while filtering out the excluded ones, resulting in higher scores. We also implemented a method that uses a single clustering on tokens, which yielded poor results. This emphasizes the importance of clustering clean components. Overall, with the addition of three extra loss functions, FDCA achieves clear disentangled features, resulting in better-fused video representations.

Table 4: Ablation studies on each loss.

Method	$\mathcal{L}^{\mathrm{S}}$	$\mathcal{L}^{\mathrm{T}}$	$\mathcal{L}_{\mathrm{R}}$	$\mathcal{L}_{\mathrm{Tri}}$	R1	R5	R10	R50
w/ SFD	✓				22.76	53.20	68.40	94.19
w/ ATD		✓			12.42	37.78	53.89	86.40
w/ SFD+ATD	✓	✓			22.15	52.66	68.13	93.83
w/ SFD+ATD		✓	✓	✓	21.37	51.59	67.42	93.89
w/ SFD+ATD	✓		✓	✓	20.83	51.56	67.35	93.85
w/ SFD+ATD	✓	✓		✓	24.42	53.94	68.95	93.78
w/ SFD+ATD	✓	✓	✓		23.17	53.36	68.23	94.00
w/ single cluster	✓	✓	✓	✓	22.01	52.46	67.96	93.81
FDCA	✓	✓	✓	✓	**25.84**	**55.84**	**70.23**	**94.33**

5.4 Analysis

Effect of Auxiliary Token Disentangling. In Figure 4, we visualize the cross-modal features obtained through the alignment module using image features from the second last layer of visual encoder. In Sample 1, we can observe that by integrating ATD, the network significantly enhances the focus on the retained component (red), *i.e.*, the `kitchen`. Moreover, the modification text is now distinguishable as retained text and injected text (blue) without the excluded text. In Sample 2, when the model lacks ATD, it concentrates wrongly at the excluded component (red), *i.e.*, the `ground`. With the help of ATD, the model shifts its focus to the action of `doing exercises`, demonstrating the essential role of ATD.

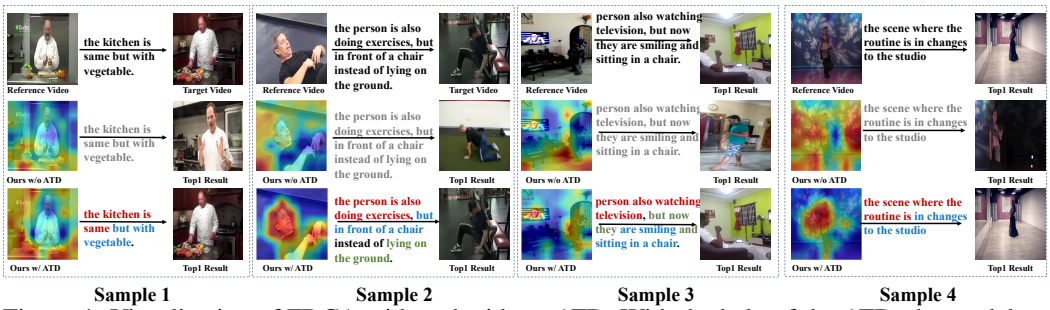

Figure 4: Visualization of FDCA with and without ATD. With the help of the ATD, the model can focus on the retained component in the reference video.

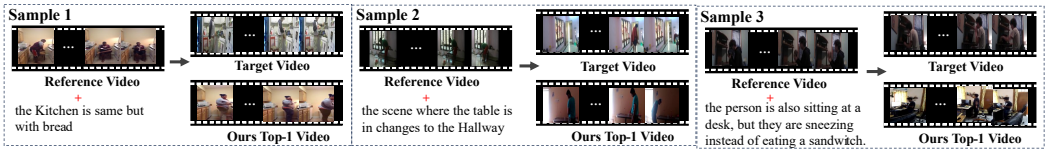

Figure 5: The visualization of bad cases.

Auxiliary Mechanism or Main Mechanism. In FDCA, the ATD exclusively participates in the training process. To maximize the utility of the features derived from ATD, we validate the performance under the prior-fusion and post-fusion settings. Prior-fusion involves the integration of features before the CMFA and CMFF, while post-fusion incorporates features subsequent to these two modules. The results in Table 5 show that our auxiliary mechanism outperforms these two fusion methods. Notably, the prior-fusion method surpasses the post-fusion. This observation suggests that features at the sentence and token level somehow exhibit redundancy, and the subsequent alignment module in the prior-fusion effectively mitigates this redundancy. In comparison, our approach directly utilizes the sentence-level feature, thereby circumventing this redundancy issue and achieving superior results.

Table 5: Results on different fusion mechanisms.

Method	R1	R5	R10	R50
Prior Fusion	25.70	**56.03**	**70.35**	94.29
Post-Fusion	23.29	53.28	68.11	93.62
FDCA	**25.84**	55.84	70.23	**94.33**

Case Studies. We analyze the bad case that ranks out of 100 via the FDCA-BLIP to show the limitation of our method and the challenge of the FineCVR-1M dataset. As depicted in Figure 5, our dataset primarily poses a significant challenge for algorithms in the need to balance visual and semantic similarity. In the first case, the retrieved video may closely resemble the reference video but might not clearly show `bread` in the first case, possibly due to the small object scale of the `bread`. In the second case, the algorithm needs to accurately understand the event `sneezing` , but our method finds a video that only performs `sitting`. This highlights the importance of temporal modeling, which involves capturing the dynamic changes in the video over time and understanding how they relate to the semantic content. Overall, addressing these challenges requires algorithms to further deal with the spurious and missing correlation in the appearance and temporal information in the video with a more elegant design.

Different Temporal Encoders. We explore three temporal encoders in Table 6. Following CLIP4Clip (Luo et al., 2022), we replace the temporal encoder with LSTM and Transformer. The results, consistent with CLIP4Clip, show that mean-pooling yields better performance. However, this doesn't imply that the input video is insignificant, as Table A7 in the Appendix shows that using only images leads to worse results. These findings suggest that a simple temporal encoder is insufficient for fine-grained temporal modeling. More advanced temporal encoders are needed to address fine-grained retrieval effectively.

Table 6: Results on different temporal encoders.

Method	R1	R5	R10	R50
FDCA-MeanP	**25.84**	**55.84**	**70.23**	**94.33**
FDCA-Trans	24.45	54.53	69.07	93.91
FDCA-LSTM	23.17	53.36	67.71	91.65

6 Conclusion

This paper introduces a new dataset FineCVR-1M to facilitate the study of fine-grained CVR and down-stream adaption of large-scale pre-trained models. Moreover, we propose a method FDCA for fine-grained CVR. FDCA extracts cross-modal fused features by disentangling text features at both the sentence and token levels regarding the reference video. Our experiments demonstrate that the dataset we create has good quality and diversity, and our method achieves remarkable performance compared to other competitors including the original pre-trained VLMs and other CVR methods. Further study includes more intriguing modeling of the complex video temporal information and integration into the multi-modal foundation model development, especially from the perspectives of fine-grained video information seeking and video-centric dialog applications.

REPRODUCIBILITY STATEMENT

To ensure the reproducibility of our work, we provide comprehensive details on datasets in Section 3 and Section B, method design in Section 4. Details of the training strategies can be found in Section A. The source code has been submitted as supplementary materials.

REFERENCES

Alberto Baldrati, Marco Bertini, Tiberio Uricchio, and Alberto Del Bimbo. Effective conditioned and composed image retrieval combining clip-based features. In *Proceedings of the IEEE/CVF Conference on Computer Vision and Pattern Recognition*, pp. 21466–21474, 2022.

Alberto Baldrati, Lorenzo Agnolucci, Marco Bertini, and Alberto Del Bimbo. Zero-shot composed image retrieval with textual inversion. *arXiv preprint arXiv:2303.15247*, 2023.

Ting Chen, Simon Kornblith, Mohammad Norouzi, and Geoffrey Hinton. A simple framework for contrastive learning of visual representations. In *International conference on machine learning*, pp. 1597–1607. PMLR, 2020a.

Yanbei Chen, Shaogang Gong, and Loris Bazzani. Image search with text feedback by visiolinguistic attention learning. In *Proceedings of the IEEE/CVF Conference on Computer Vision and Pattern Recognition*, pp. 3001–3011, 2020b.

Yiyang Chen, Zhedong Zheng, Wei Ji, Leigang Qu, and Tat-Seng Chua. Composed image retrieval with text feedback via multi-grained uncertainty regularization. *arXiv preprint arXiv:2211.07394*, 2022.

Ginger Delmas, Rafael Sampaio de Rezende, Gabriela Csurka, and Diane Larlus. Artemis: Attention-based retrieval with text-explicit matching and implicit similarity. *arXiv preprint arXiv:2203.08101*, 2022.

Ali Diba, Mohsen Fayyaz, Vivek Sharma, Manohar Paluri, Jürgen Gall, Rainer Stiefelhagen, and Luc Van Gool. Large scale holistic video understanding. In *Computer Vision–ECCV 2020: 16th European Conference, Glasgow, UK, August 23–28, 2020, Proceedings, Part V 16*, pp. 593–610. Springer, 2020.

Eric Dodds, Jack Culpepper, Simao Herdade, Yang Zhang, and Kofi Boakye. Modality-agnostic attention fusion for visual search with text feedback. *arXiv preprint arXiv:2007.00145*, 2020.

Mingjing Du, Shifei Ding, and Hongjie Jia. Study on density peaks clustering based on k-nearest neighbors and principal component analysis. *Knowledge-Based Systems*, 99:135–145, 2016.

Bernard Ghanem Fabian Caba Heilbron, Victor Escorcia and Juan Carlos Niebles. Activitynet: A large-scale video benchmark for human activity understanding. In *Proceedings of the IEEE Conference on Computer Vision and Pattern Recognition*, pp. 961–970, 2015.

Xintong Han, Zuxuan Wu, Phoenix X. Huang, Xiao Zhang, Menglong Zhu, Yuan Li, Yang Zhao, and Larry S. Davis. Automatic spatially-aware fashion concept discovery. In *ICCV*, 2017.

Mehrdad Hosseinzadeh and Yang Wang. Composed query image retrieval using locally bounded features. In *Proceedings of the IEEE/CVF Conference on Computer Vision and Pattern Recognition*, pp. 3596–3605, 2020.

Edward J Hu, Yelong Shen, Phillip Wallis, Zeyuan Allen-Zhu, Yuanzhi Li, Shean Wang, Lu Wang, and Weizhu Chen. Lora: Low-rank adaptation of large language models. *arXiv preprint arXiv:2106.09685*, 2021.

Thomas Hummel, Shyamgopal Karthik, Mariana-Iuliana Georgescu, and Zeynep Akata. Egocvr: An egocentric benchmark for fine-grained composed video retrieval. *arXiv preprint arXiv:2407.16658*, 2024.

Jingwei Ji, Ranjay Krishna, Li Fei-Fei, and Juan Carlos Niebles. Action genome: Actions as compositions of spatio-temporal scene graphs. In *Proceedings of the IEEE/CVF Conference on Computer Vision and Pattern Recognition*, pp. 10236–10247, 2020.

Peng Jin, Jinfa Huang, Pengfei Xiong, Shangxuan Tian, Chang Liu, Xiangyang Ji, Li Yuan, and Jie Chen. Video-text as game players: Hierarchical banzhaf interaction for cross-modal representation learning. In *Proceedings of the IEEE/CVF Conference on Computer Vision and Pattern Recognition*, pp. 2472–2482, 2023a.

Peng Jin, Hao Li, Zesen Cheng, Jinfa Huang, Zhennan Wang, Li Yuan, Chang Liu, and Jie Chen. Text-video retrieval with disentangled conceptualization and set-to-set alignment. *arXiv preprint arXiv:2305.12218*, 2023b.

Giorgos Kordopatis-Zilos, Symeon Papadopoulos, Ioannis Patras, and Ioannis Kompatsiaris. Visil: Fine-grained spatio-temporal video similarity learning. In *Proceedings of the IEEE/CVF international conference on computer vision*, pp. 6351–6360, 2019.

Seungmin Lee, Dongwan Kim, and Bohyung Han. Cosmo: Content-style modulation for image retrieval with text feedback. In *Proceedings of the IEEE/CVF Conference on Computer Vision and Pattern Recognition*, pp. 802–812, 2021.

Hao Li, Yanhao Jia, Peng Jin, Zesen Cheng, Kehan Li, Jialu Sui, Chang Liu, and Li Yuan. Freestyleret: Retrieving images from style-diversified queries. In *European Conference on Computer Vision*, pp. 258–274. Springer, 2024.

Junnan Li, Dongxu Li, Caiming Xiong, and Steven Hoi. Blip: Bootstrapping language-image pre-training for unified vision-language understanding and generation. In *International Conference on Machine Learning*, pp. 12888–12900. PMLR, 2022.

Junnan Li, Dongxu Li, Silvio Savarese, and Steven Hoi. Blip-2: Bootstrapping language-image pre-training with frozen image encoders and large language models. *arXiv preprint arXiv:2301.12597*, 2023.

Zheyuan Liu, Cristian Rodriguez, Damien Teney, and Stephen Gould. Image retrieval on real-life images with pre-trained vision-and-language models. In *ICCV*, 2021.

Huaishao Luo, Lei Ji, Ming Zhong, Yang Chen, Wen Lei, Nan Duan, and Tianrui Li. Clip4clip: An empirical study of clip for end to end video clip retrieval and captioning. *Neurocomputing*, 508: 293–304, 2022.

Long Ouyang, Jeffrey Wu, Xu Jiang, Diogo Almeida, Carroll Wainwright, Pamela Mishkin, Chong Zhang, Sandhini Agarwal, Katarina Slama, Alex Ray, et al. Training language models to follow instructions with human feedback. *Advances in Neural Information Processing Systems*, 35: 27730–27744, 2022.

Alec Radford, Jong Wook Kim, Chris Hallacy, Aditya Ramesh, Gabriel Goh, Sandhini Agarwal, Girish Sastry, Amanda Askell, Pamela Mishkin, Jack Clark, et al. Learning transferable visual models from natural language supervision. In *International conference on machine learning*, pp. 8748–8763. PMLR, 2021.

Kuniaki Saito, Kihyuk Sohn, Xiang Zhang, Chun-Liang Li, Chen-Yu Lee, Kate Saenko, and Tomas Pfister. Pic2word: Mapping pictures to words for zero-shot composed image retrieval. In *Proceedings of the IEEE/CVF Conference on Computer Vision and Pattern Recognition*, pp. 19305–19314, 2023.

Omkar Thawakar, Muzammal Naseer, Rao Muhammad Anwer, Salman Khan, Michael Felsberg, Mubarak Shah, and Fahad Shahbaz Khan. Composed video retrieval via enriched context and discriminative embeddings. In *Proceedings of the IEEE/CVF Conference on Computer Vision and Pattern Recognition*, pp. 26896–26906, 2024.

Hugo Touvron, Thibaut Lavril, Gautier Izacard, Xavier Martinet, Marie-Anne Lachaux, Timothée Lacroix, Baptiste Rozière, Naman Goyal, Eric Hambro, Faisal Azhar, et al. Llama: Open and efficient foundation language models. *arXiv preprint arXiv:2302.13971*, 2023a.

Hugo Touvron, Louis Martin, Kevin Stone, Peter Albert, Amjad Almahairi, Yasmine Babaei, Nikolay Bashlykov, Soumya Batra, Prajjwal Bhargava, Shruti Bhosale, et al. Llama 2: Open foundation and fine-tuned chat models. *arXiv preprint arXiv:2307.09288*, 2023b.

Lucas Ventura, Antoine Yang, Cordelia Schmid, and Gül Varol. Covr: Learning composed video retrieval from web video captions. In *Proceedings of the AAAI Conference on Artificial Intelligence*, volume 38, pp. 5270–5279, 2024.

Nam Vo, Lu Jiang, Chen Sun, Kevin Murphy, Li-Jia Li, Li Fei-Fei, and James Hays. Composing text and image for image retrieval-an empirical odyssey. In *Proceedings of the IEEE/CVF conference on computer vision and pattern recognition*, pp. 6439–6448, 2019.

Qiang Wang, Yanhao Zhang, Yun Zheng, Pan Pan, and Xian-Sheng Hua. Disentangled representation learning for text-video retrieval. *arXiv preprint arXiv:2407.16658*, 2022. URL `https://arxiv.org/abs/2203.07111`.

Haokun Wen, Xuemeng Song, Xin Yang, Yibing Zhan, and Liqiang Nie. Comprehensive linguistic-visual composition network for image retrieval. In *Proceedings of the 44th International ACM SIGIR Conference on Research and Development in Information Retrieval*, pp. 1369–1378, 2021.

Hui Wu, Yupeng Gao, Xiaoxiao Guo, Ziad Al-Halah, Steven Rennie, Kristen Grauman, and Rogerio Feris. The fashion iq dataset: Retrieving images by combining side information and relative natural language feedback. *CVPR*, 2021.

Jiarui Xu and Xiaolong Wang. Rethinking self-supervised correspondence learning: A video frame-level similarity perspective. In *Proceedings of the IEEE/CVF International Conference on Computer Vision*, pp. 10075–10085, 2021.

Jun Xu, Tao Mei, Ting Yao, and Yong Rui. Msr-vtt: A large video description dataset for bridging video and language. In *Proceedings of the IEEE conference on computer vision and pattern recognition*, pp. 5288–5296, 2016.

Wang Zeng, Sheng Jin, Wentao Liu, Chen Qian, Ping Luo, Wanli Ouyang, and Xiaogang Wang. Not all tokens are equal: Human-centric visual analysis via token clustering transformer. In *Proceedings of the IEEE/CVF Conference on Computer Vision and Pattern Recognition*, pp. 11101–11111, 2022.

In this Appendix, we provide:

1. More experiments in Section A.
2. More details and samples of the FineCVR-1M dataset in Section B.

A EXPERIMENTS

A.1 EXPERIMENTAL SETUP

Baseline Methods. To assess the necessity of this CVR paradigm, we evaluate the following baselines by a frozen CLIP:

- Video-only uses the reference video as input only.
- Text-only queries by the modification text.
- Video-text sum is to sum the reference video feature and modified text feature from CLIP directly.
- Linear layer is to employ a linear layer to compose the features of the reference video and modification text from CLIP or BLIP.

Composed Query Retrieval Methods. As there are currently no existing methods specifically designed to solve the CVR task, we compare our FDCA with several reproduced composed query retrieval methods as follows:

- TIRG (Vo et al., 2019) employs a gated module and a residual module to learn the transformation and preservation features.
- MAAF (Dodds et al., 2020) introduces a self-attention model to enhance the interaction of the cross-modality features.
- CosMo (Lee et al., 2021) uses content and style modulators to learn the underlying style information and residual information.
- Uncertainty-R (Chen et al., 2022) extracts the multi-grained feature and introduces uncertainty regularization to adapt the matching objective.
- Artemis (Delmas et al., 2022) sums the implicit similarity and explicit match scores to produce the final score for retrieval.
- Pic2word (Saito et al., 2023) transforms an input image to a language token, then composes the pseudo token with text tokens through 3 fully-connection layers to obtain the fused feature.
- Combiner (Baldrati et al., 2022) contains 5 linear layers to combine the two modalities feature from the CLIP features.
- FreestyleRet (Li et al., 2024) propose style-space construction and a prompt-tuning strategy structure.
- CoVR (Ventura et al., 2024) finetunes the text encoder of the BLIP model directly.
- TFR-CVR (Hummel et al., 2024) use an LLM to combine the video caption and textual modifier into a coherent target caption.

We reproduce all the compared methods in the CVR paradigm by inputting a video and a text. To encode videos that have an additional temporal dimension, **we utilize mean-pooling in the temporal dimension as the temporal encoder for all the compared methods**.

Implementation Details. All experiments are conducted on the NVIDIA RTX3090 using PyTorch. For our proposed method FDCA, we utilize the frozen CLIP Res50x4 ($d = 640$) (Radford et al., 2021) or BLIP large ($d = 256$) (Li et al., 2022) as our video encoder. The model is optimized with Adam with an initial learning rate of 1e-4. We set the batch size to 1024 to maintain the performance. To avoid overfitting, we train our FDCA for 30 epochs. The m in the triplet loss $\mathcal{L}_{\text{Tri}}$ is 0.2, while the weight λ of the triplet loss $\mathcal{L}_{\text{Tri}}$ is set as 5. We implement the Cross-Modality Feature Alignment (CFA) and Cross-Modality Feature Fusion (CFF) modules using six Transformer Encoder layers.

Table A7: Results of Different Query for Video Retrieval on FineCVR-1M test dataset.

Train/Val	Test	R1	R5	R10	R50
img+mod	img+mod	20.51	43.19	60.71	90.12
	vdo+mod	22.18	45.82	63.92	91.80
vdo+mod	img+mod	15.00	37.10	49.32	76.88
	vdo+mod	**25.84**	**55.84**	**70.23**	**94.33**

Table A8: Results on WebVid-CoVR test dataset.

Method	Finetuned BLIP's text encoder	R1	R5	R10	R50
CoVR	✓	53.13	79.93	86.85	**97.69**
FDCA-BLIP		52.23	79.42	86.66	96.91
FDCA-BLIP	✓	**53.34**	**80.23**	**88.28**	97.45

Each encoder layer consists of a multi-head attention mechanism, a Layer Normalization (LayerNorm), and a Feed-Forward Network (FFN).

A.2 Results on Different Query for Video Retrieval

To explore the relative effectiveness of images and videos in the CVR task, we conduct validations on the FineCVR-1M test dataset using queries that included modification text either composed with an image (img+mod) or a video (vdo+mod). The image is the middle frame of the video. As shown in Table A7, due to the rich action descriptions in our dataset, whether trained with image+mod or video+mod, the test results for image+mod were comparatively lower. This indicates that the visual information provided by a single image is insufficient to convey complete semantic information. In contrast, videos can not only provide more comprehensive visual information but also offer fine-grained contextual information, making the performance of vdo+mod better.

A.3 Results on Other CVR Datasets

WebVid-CoVR-Test Dataset: We employ the CoVR and FDCA-BLIP for training and testing on the WebVid-CoVR dataset, and the results are shown in Table A8. The results for CoVR are from the paper (Ventura et al., 2024). It can be observed that our method is slightly inferior to directly fine-tuned CoVR. This may be due to the fact that modification texts in the WebVid-CoVR dataset are often incomplete sentences, which hinders the provision of the three essential components, consequently impacting the effectiveness of the FDCA method. Additionally, CoVR employs the fine-tuned BLIP directly, while our FDCA only utilizes the frozen BLIP. This may be another reason why ours is slightly inferior to CoVR. Therefore, we adjust our training strategy by reducing the weight $\lambda = 1$ of L_T, setting $m = 0.05$, and fine-tuning BLIP's text encoder following CoVR's configuration. These modifications led to improved performance.

EgoCVR Test Dataset: We also validate our method on the EgoCVR dataset (Hummel et al., 2024). Due to the unavailability of training data, we directly apply our FDCA-BLIP model pretrained on VCCR-1M for testing. The results are presented in Table A9. TFR-CVR (Hummel et al., 2024) achieves superior performance as it leverages pre-trained video-language weights from the EgoCVR dataset and requires no additional training. In contrast, both our method and CoVR require training but lack access to the training set, resulting in relatively lower performance. Nevertheless, our approach still outperforms CoVR, particularly on the fine-grained R1 metric, demonstrating the effectiveness of our decomposition strategy in fine-grained retrieval tasks.

MSRVTT-1K Test Dataset: The CVR task contains text that describes specific modifications to videos. Hence, our FDCA uses reference videos as guidance to separate and identify meaningful components for alignment and fusion. However, text in text-video retrieval matches with the content of the video. This makes our disentanglement approach unsuitable for the general text-video retrieval task directly. To validate the effectiveness of disentanglement for alignment, we extend

Table A9: Results on Ego-CVR test dataset.

Method	Global			Local		
	R1	R5	R10	R1	R5	R10
CoVR (Ventura et al., 2024)	5.4	15.2	24.3	33.1	49.5	62.9
FDCA-BLIP	8.7	19.2	27.1	36.3	51.1	63.8
TFR-CVR (Hummel et al., 2024)	**14.1**	**39.5**	**54.4**	**44.2**	**61.0**	**73.2**

Table A10: Performance on MSRVTT-1K dataset.

Method	Text-to-video			Video-to-text		
	R1	R5	R10	R1	R5	R10
CLIP4Clip (Luo et al., 2022)	44.5	71.4	81.6	42.7	70.9	80.6
WTI (Wang et al., 2022)	47.4	74.6	83.8	45.3	73.9	83.3
Ours	**48.7**	**75.2**	**84.5**	**46.4**	**74.6**	**83.6**

the WTI (Wang et al., 2022) by decomposing text features into three components using our FDCA. Each component is weighted with video token features for alignment. We train this method based on WTI with $\mathcal{L}^{\mathrm{S}}$ and $\mathcal{L}^{\mathrm{T}}$. The general text-video retrieval results on MSRVTT-1K (Xu et al., 2016) are shown in Table A10.

A.4 Parameter Sensitivity

In the ATD, we leverage a triplet loss $\mathcal{L}_{\mathrm{Tri}}$ to penalize the presence of negation semantics in videos. We study the effects of two parameters including m and λ in the triplet loss $\mathcal{L}_{\mathrm{Tri}}$ on the FineCVR-1M validation set.

Effect of m. m is the margin value between positive samples and negative samples. As shown in Figure A6a, while the performance variations across different margins m are small in our FineCVR-1M dataset, there is a decline in performance as m increases. The best performance's m is located at $m = 0.2$, which is used in our method. This underscores the effectiveness of our ATD in generating negative samples to filter misleading information.

Effect of λ. λ is the weight of triplet loss $\mathcal{L}_{\mathrm{Tri}}$. From Figure A6b, it can be seen that the weight of the triplet loss has a minor impact on the final results. Finally, we choose a parameter that yields consistently good overall performance, with $\lambda = 5$. This choice ensures the highest effectiveness for both R10 and R50, while also delivering satisfactory results for R1 and R5.

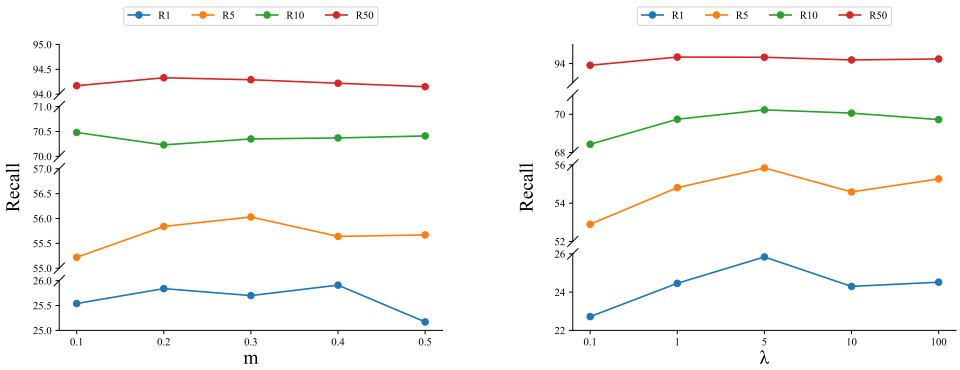

(a) Result of different m.

(b) Results of different λ

Figure A6: The analysis of parameters in the triplet loss. (a) Effect of m. (b) Effect of λ

Table A11: Performance on three components by ATD.

Retained	Injected	Excluded	R1	R5	R10	R50
✓			18.20	42.98	60.12	89.10
✓	✓		24.15	53.29	68.91	92.96
✓	✓	✓	**25.84**	**55.84**	**70.23**	**94.33**

Table A12: Results on better temporal encoding mechanism.

Method	R1	R5	R10	R50
FDCA-Trans	24.45	54.53	69.07	93.91
FDCA-Trans-Dicosa (Jin et al., 2023b)	25.18	51.12	64.07	90.25
FDCA-Trans-Dicosa+retained	**25.79**	**55.90**	**69.94**	**94.05**

A.5 The Importance of Three Components

The FDCA with ATD only can decompose the token into three components including retained, injected, and excluded components. Hence, to explore the importance of the three components, we ablate each component in the final fusion module. Table A11 shows that all three components are essential. The performance with retained components is not bad, since the retained components can make the model focus on the target video which is similar to the retained video feature. Moreover, when the injected component is introduced, the model can produce a fused video feature that meets the modified needs of the user. Furthermore, with the help of the excluded component, the model can filter the results that the user doesn't want. All these components help the model understand the visual and semantic demands of users clearly.

A.6 Exploration of Better Temporal Encoder

Intuitively, since video composed retrieval requires understanding contextual information within videos, incorporating a superior temporal encoder would yield better results. Here, we employ the temporal encoding mechanism in DiCoSA (Jin et al., 2023b) in Table A12. Its effectiveness is limited to R1 metrics. We believe this limitation arises because DiCoSA's text information, which directly corresponds to video content, can be aligned with videos for weighted sum computation. In contrast, our text information contains modification-related semantics, and using weighted sums introduced certain biases. When we instead use our decomposed residual features for weighted sum computation, we observed significant performance improvements. This validates both the effectiveness of our decomposition approach and demonstrates that superior temporal encoders can enhance temporal understanding.

A.7 Comparison of training and inference performance.

We compare training time in Table A13, and inference time in Table A14. Although our model has the most parameters, it converges faster and has a faster inference speed. Since we only use SFD during the inference stage, the inference speed is only slightly slower than the Combiner (Baldrati et al., 2022).

Table A13: Training time comparison.

Method	Parms	Processed data	Epoch	Training time per epoch	Total time
CoVR (Ventura et al., 2024)	446M	Image	5	30 h	150 h
Pic2word (Saito et al., 2023)	179M	CLIP feature	30	6 min	3 h
Combiner (Baldrati et al., 2022)	237M	CLIP feature	100	10 min	16 h
FDCA	570M	CLIP feature	30	20 min	10 h

Table A14: Inference time comparison.

Method	Parms	Processed data	Inference time per
CoVR (Ventura et al., 2024)	446M	Image	56 pairs/s
Pic2word (Saito et al., 2023)	179M	Image	149 pairs/s
Combiner (Baldrati et al., 2022)	237M	Image	107 pairs/s
FDCA	570M	Image	84 pairs/s

A.8 Visualization of ATD

We offer some illustrative examples of ATD results in Figure A7. As observed, ATD can effectively disentangle the modification text into three distinct components: clean retained tokens, injected tokens, and excluded tokens. Because we guide the disentangling of initial retained tokens through reference video features, the tokens are typically crucial retained components in the reference video, such as concepts like `..bathroom.. but rearranging on the sink` in the first example and `.. singing, but..` in the seventh example. On the other hand, the injected tokens are the remaining parts of the modification text. Therefore, injected tokens usually include concepts from the target video as well as grammatical elements, such as and `the person is also in .. the takes a pill .. objects` in the first example and `the .. is .. with net` in the sixth example. After the Fine Clustering, the initial retained token can be disentangled into clean retained tokens `bathroom` and excluded tokens `but rearranging on the sink`. Notably, even in the modification text without negation words, the ATD can also detect the excluded tokens such as the `boy` that should not exist in the target video in the fourth example.

B The FineCVR-1M Dataset

As shown in Figure A8, we first match similar videos as the reference video and the target video, respectively. We then automatically generate modification texts regarding static concepts and action concepts, respectively. The former generates modification texts by filling the different key static concepts into the textual prompts, while the latter leverages a fine-tuned LLM to generate the action difference description directly.

B.1 Video Preprocess and Pairing.

We begin by extracting videos from public datasets and clipping them based on event timestamps provided in the annotations. Videos without annotations are excluded from the dataset.

We establish video pairs from the same video source by utilizing cosine similarity, a widely used metric in video similarity learning (Kordopatis-Zilos et al., 2019; Xu & Wang, 2021; Chen et al., 2020a). Specifically, we uniformly sample 8 frames from each video and compute their frame-level features using BLIP-2 (Li et al., 2023). These features are then mean-pooled to obtain a compact video-level representation. Using cosine similarity between compact video features to compute video similarity, we identify the top 20 most similar videos for each query video, forming pairs that serve as the foundation for subsequent text modification text generation. To further ensure dataset quality, we instruct annotators to exclude irrelevant video pairs during test set construction.

B.2 Modification Text Generation

For static concepts, we use fixed templates to generate differences and similarities among key concepts. To ensure the high quality of the static concepts, concepts in our FineCVR-1M dataset are obtained from the annotations and captions of four accessible benchmark datasets (Ji et al., 2020), as well as high-confidence score results by BLIP. Figure A9 illustrates the detailed process of key object calculation. In detail, objects in the caption are more semantically meaningful for humans and represent key concepts, thus receiving higher scores of 1.0. Object annotation is also critical for this task, so we give it 0.5. We believe that the results from BLIP provide basic visual information with low confidence, so we assign a score of 0.1 to the BLIP result. Moreover, the importance of

Reference Video & Target Video	Mod Text	Initial Retained Positive Tokens	Injected (Positive) Tokens	Initial Retained Tokens	Clean Retained (Positive) Tokens	(Clean) Excluded Tokens	Excluded Tokens w/ Negation Words
	the person is also in the bathroom, but takes a pill instead of rearranging objects on the sink.	.. bathroom .. but rearranging on the sink	the person is also in .. the takes a pill .. objects	bathroom .. but instead of rearranging on the sink	..bathroom..	but rearranging on the sink	but instead of rearranging on the sink
	the home office / study is same but with laptop	office study .. same but ..	the home .. is .. with laptop	office study .. same but ..	.. office study .. same but ..	-	-
	the Living room is same but with a broom	the living room .. same but ..	is .. with a broom ..	the living room .. same but ..	the living room .. same but ..	-	-
	the person changes from a boy to a woman	.. boy to a ..	the person changes from a .. woman	.. boy to a ..	.. to a ..	.. boy ..	.. boy ..
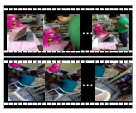	the Home Office / Study is same but with chair	.. office / study .. same but ..	the home .. is .. with chair	office / study .. same but ..	office / study .. same	.. but ..	.. but ..
	the arena is same but with net	.. arena .. same but ..	the .. is .. with net	.. arena.. but	.. arena same..	..but..	..but..
	the person is also singing, but on the show with a good judge	.. singing , but ..	the person is also .. on the show with a good judge	.. singing , but..	..singing..	..but..	..but..
	the scene where the vacuum is in changes to the Kitchen	.. vacuum is in changes to ..	the scene where the.. the kitchen	.. vacuum is in changes to ..	vacuum is .. to ..	.. in changes ..	.. in changes ..
	the person takes another shot and makes it and we see a recap of that as well	.. shot and .. and .. that..	the person takes another .. makes it .. we see a recap of .. as well	.. shot and .. and .. that ..	.. shot and .. and .. as..	.. we ..	.. we ..
	the person is also spreading something on bread, but it has changed to butter instead of mustard	.. spreading .. on bread .. but .. to ..	the person is also .. something .. it has changed .. butter	.. spreading .. on bread , but .. to .. instead of mustard	.. spreading .. on .. but .. to mustard	.. instead of bread ..	.. bread ..

Figure A7: Examples of ATD results.

words in the caption is related to their location, with the last word being less important than the first word. Hence, we assign the first object in the caption list as the highest location score, and the last object a location score of 0. In summary, our FineCVR-1M dataset benefits from the utilization of these four reliable sources of data, resulting in a dataset with high-quality key concepts.

Then we compare key static concepts between video pairs and generate descriptions of their differences with three types of prompts: **(a)** identify the scene difference where the same object appears

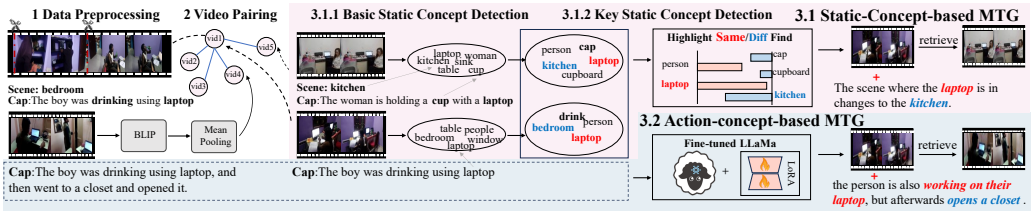

Figure A8: Pipeline of dataset construction. We segment long videos into video clips by Preprocessing and pairing video clips by similarity comparison. Then we use prompts and LLM to generate modification texts regarding static concepts and action concepts, respectively.

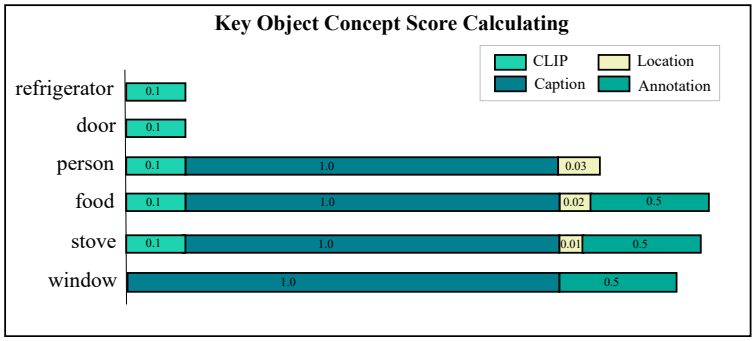

Figure A9: A sample of calculating key object scores. The caption is "a person cooks food on a stove before looking out of a window", and the CLIP detects that there are [refrigerator, door, person, food] in this video. The objects in the caption are [person, food, stove, window], and the objects in the annotation are [food, stove, window]. After calculating, the key object is "food" with the highest score of 1.62.

in the video pair like *"the scene where the* {***} *is in changes to the* {***}*"*; **(b)** choose a different object as the focus of the prompt for videos with the same scene, formed as *"the* {***} *is same but with* {***}*"*; and **(c)** replace the attributes of the object in the target video when the key object concept is the same, *e.g.*, *"the attribute of the* {***} *is replaced by* {***}*"*.

Furthermore, to explore the impact of fixed templates, we also rewrite 6,043 sample texts using GPT-4 for the test set. Table A15 shows that flexible texts have a minimal impact on results, since the CLIP or BLIP text encoder is robust enough to comprehend the core semantic meaning. Moreover, the gap between the FDTA-CLIP is bigger than that between the FDTA-BLIP, which could be attributed to the BLIP encoder being BERT, capable of handling complex sentences. This indicates that for a superior text encoder, the flexibility of the text will have little impact on the results as long as the core content remains consistent.

Table A15: Test result on rewritten flexible modification text by GPT-4.

Method	Dataset	R1	R5	R10	R50
FDTA-CLIP	FineCVR-1M	14.69	46.17	64.87	94.44
	Rewritten	14.23	43.31	61.91	92.45
FDTA-BLIP	FineCVR-1M	**18.68**	**52.39**	**70.99**	**95.28**
	Rewritten	18.08	51.32	70.23	94.89

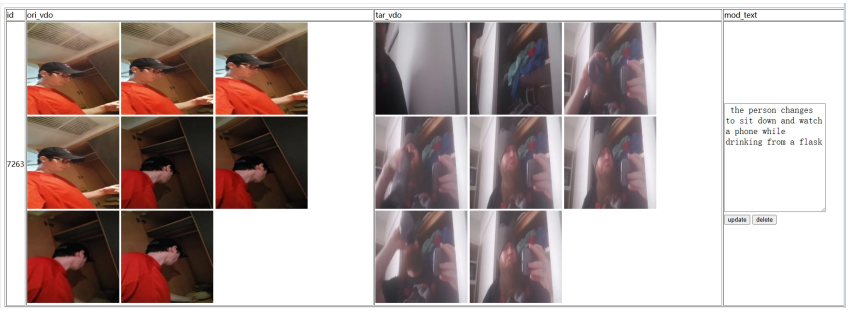

Figure A10: We manually select samples that have visual differences and similarities.

Table A16: The statistics of the prompt class in the dataset.

ClsID	Method	Prompt	Coverage	Example
(a)	Static-Concept	*the scene where the* {***} *is in changes to the* {***}	28.54%	the scene where the *bag* is in changes to the *entryway*
(b)		*the* {***} *is same but with* {***}	22.08%	the *bedroom* is same but with *screen*
(c)		*the attribute of the* {***} *is replaced by* {***}	0.48%	the attribute of the *blanket* is replaced by *throw*
(d)	Action-Concept	I'll give two video captions, and you should compare theses	11.70%	the person is *cooking at the stove*, but *looks for something inside frige*
(e)		and complete change captioning based on something same	37.20%	the person changes to *pick up clothes instead of shaking a blanket out*

(a) (b) (c) (d) (e)

For action concepts, we use LLM to generate differences and similarities between video caption pairs. We first attempt to use ChatGPT (Ouyang et al., 2022) to generate 1,000 data samples for validation. Specifically, we input the following prompt with caption pairs into ChatGPT to generate 1000 samples into **(d)** different actions with similarities and **(e)** different actions:

> I'll give two ordered video captions, and you should compare two videos and complete a change captioning task based on something similar and return to me with a concluded sentence as the following template. If the same action or object or event exists in both two ordered videos, you should fill this same thing in the first {} and output: "the person is also {} in both two videos, but {} in the second video ". Else you output: "The person changes to {} in the second video". (please check carefully, if you use the first format, there must be something that exists in both videos). Only give me an output as one of the above formats.

However, we find that the accuracy was not high (below 60%) since ChatGPT had not previously encountered this type of task. To ensure that the LLM could effectively adapt to identifying differences and similarities between video caption pairs, we manually revise the responses of the 1,000 samples. We then used 606 samples as a training set and 394 as a validation set to fine-tune the open-source model LLaMA 2 (Touvron et al., 2023b). As a result, we achieve an accuracy of 92% and used this fine-tuned model to generate the action concepts text.

Additionally, we observed that despite instructing the LLM to generate two categories: **(d)** and **(e)**, it still tends to hallucinate similarities that do not actually exist. To address this, we filter out any triplets where the verbs in the identified similarities were not present in the original video captions.

For the test set, we manually select samples on the website as shown in Figure A10 that visually exhibit significant differences, ensuring they are suitable for evaluation. A user group of eight individuals, including some of the authors, is employed to ensure that the generated texts accurately reflect changes between the videos. We also implement a two-round cross-validation process. After completing the manual correction process, we obtain a gallery of 7,809 videos.

B.3 The Properties of FineCVR-1M Dataset

We summarize two properties and challenges of our FineCVR-1M as follows.

(a) (b) (c) (d) (e)

Figure A11: The word cloud of each class in our dataset.

Variable Concepts. As mentioned in the main paper, we focus on key concepts in videos in the FineCVR-1M dataset construction. Our FineCVR-1M dataset covers four different concept categories, *i.e.* objects, scenes, attributes, and actions. Comprising five types of prompts, the FineCVR-1M dataset's class coverage is detailed in Table A16. Notably, data from Static-Concept-based MTG and Action-Concept-based MTG roughly account for half of the entire dataset. This indicates that our dataset not only encompasses visual concepts but also integrates rich temporal information. For each class, we also provide a word cloud in Figure A11. Specifically, in the (a) and (b) classes, our FineCVR-1M dataset focuses on common outdoor or indoor scenes such as `sky`, along with nouns representing objects `food`, or elements associated with these scenes `window`. In the (c) class, people pay more attention to the color of objects, such as `brown hair`, and at the same time, some ongoing actions also become specific attributes of objects, such as `connecting computer`. Meanwhile, in the (d) and (e) classes, all the words revolve around human and object actions, such as `playing ball`, showcasing the diversity of actions.

Fine-grained Demand Semantic. Compared to the incomplete sentences in existing composed query datasets (Vo et al., 2019; Han et al., 2017; Liu et al., 2021; Wu et al., 2021; Ventura et al., 2024), the modification texts in our FineCVR-1M dataset are all complete sentences. Figure A12a indicates that the length of the modification text in most cases is 11 words, which is longer than the 5 words observed in the WebVid-CoVR dataset (Ventura et al., 2024). As shown in Figure A12b, our dataset covers nouns, verbs, adjectives, and even adverbs, leading the modification text to represent the complete preference of users. Moreover, we statistics the portion of three components including retained, injected, and excluded components. In FineCVR-1M, 100% modification texts comprise retained components and injected components, and 11.67% texts comprise excluded components. While the abbreviated text in Webvid-CoVR only comprises 77.68%, 100%, and 2.80%, respectively. Due to the rich information in our video, such as multiple individuals, complete semantics and rich components can prevent ambiguity caused by a lack of subject and avoid returning inaccurate video results.

The Challenges. The main challenge of our FineCVR-1M dataset is threefold: extracting concepts from videos exhaustively, understanding the semantics of modification text accurately, and fusing the cross-modal feature adequately. Videos from our FineCVR-1M not only involve static concepts but also encompass actions. Therefore, addressing the first challenge requires CVR algorithms to employ an enhanced visual encoder. The visual encoder is capable of effectively detecting concepts, even for small-scale objects and attributes. Additionally, a robust temporal encoder is essential to comprehend the semantic information conveyed by the videos. The second challenge requires algorithms with a powerful text encoder to comprehend modification text, including extracting negation meanings and capturing fine-grained words that represent users' demands. The third challenge involves developing algorithms that can integrate valuable information from both videos and modification texts. These algorithms should discern which parts in reference videos to preserve and which parts to transform, ensuring an optimal fusion of cross-modal features.

B.4 More Samples in FineCVR-1M

We present some examples from our FineCVR-1M dataset in Figure A13. Thanks to the combined insights from BLIP results, annotations, and fine-tuned LLM, our FineCVR-1M dataset offers a rich blend of concepts including static concepts and actions, showcasing elements like `stairs` and `personal protective equipment`. Additionally, the video captions provide fine-grained

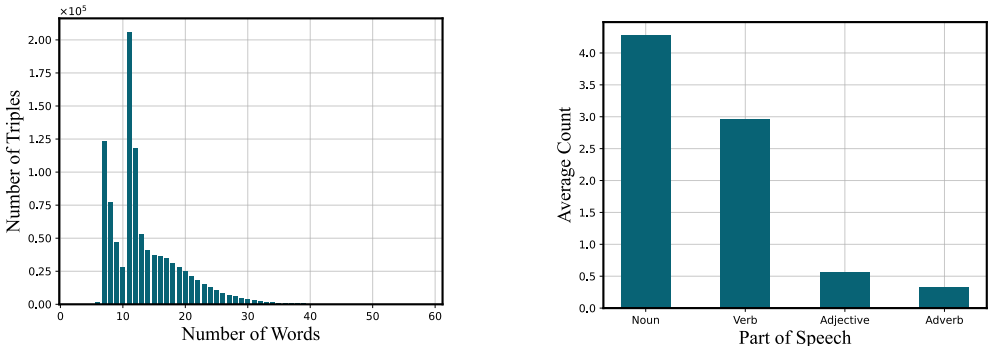

(a) The statistics of number of words.

(b) Results of different λ

Figure A12: The statistics of modification text. (a) We count the number of words for each modification text. Most modification texts have between 7 and 13 words. (b) We calculate the number of the part of speech in each modification text.

information on action changes, capturing details like `giving a hula` and `spins two hula rings`.

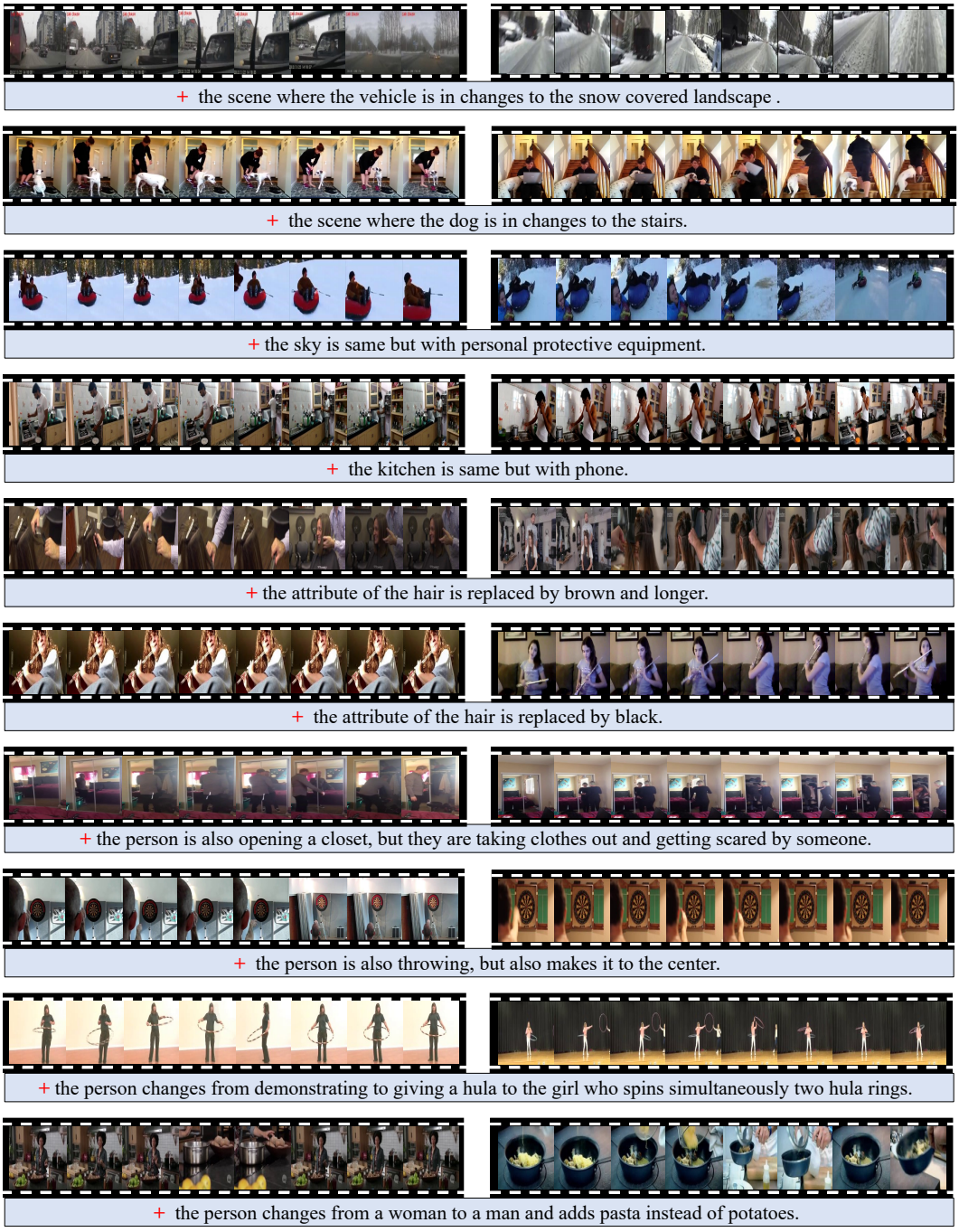

Figure A13: Example tuples in FineCVR-1M dataset. The videos on the left represent reference videos, while those on the right represent target videos. The modification texts at the bottom highlight the differences between the two videos.